4-8-2013

Correct Spectral Conversion between Surface-Enhanced Raman and Plasmon Resonance Scattering from Nanoparticle Dimers for Single-Molecule Detection

Kyuwan Lee
Birck Nanotechnology Center, Purdue University, lee70@purdue.edu

Joseph Irudayaraj
Birck Nanotechnology Center, Purdue University, josephi@purdue.edu

Lee, Kyuwan and Irudayaraj, Joseph, "Correct Spectral Conversion between Surface-Enhanced Raman and Plasmon Resonance Scattering from Nanoparticle Dimers for Single-Molecule Detection" (2013). *Birck and NCN Publications.* Paper 1384.
http://dx.doi.org/10.1002/smll.201201985

Correct Spectral Conversion between Surface-Enhanced Raman and Plasmon Resonance Scattering from Nanoparticle Dimers for Single-Molecule Detection

*Kyuwan Lee and Joseph Irudayaraj**

Simultaneous measurement of surface-enhanced Raman scattering (SERS) and localized surface plasmon resonance (LSPR) in nanoparticle dimers presents outstanding opportunities in molecular identification and in the elucidation of physical properties, such as the size, distance, and deformation of target species. SERS–LSPR instrumentation exists and has been used under limited conditions, but the extraction of SERS and LSPR readouts from a single measurement is still a challenge. Herein, the extraction of LSPR spectra from SERS signals is reported and a tool for measuring the interparticle distance from Raman enhancement data by the standardization of the SERS signal is proposed. The SERS nanoruler mechanism incorporates two important aspects (the LSPR scattering peak shift and the Raman shift for measuring interparticle distance), and signifies their exact one-to-one correspondence after spectral correction. The developed methodology is applied to calculate the interparticle distance between nanoparticle dimers from SERS signals, to detect and quantify DNA at the single-molecule level in a base-pair-specific manner. It is also shown that the SERS nanoruler concept can be used in structural analysis for the specific detection of the interaction of immunoglobulin G (IgG) with its target from bianalyte Raman signals with identical shaping at single-molecule resolution. The SERS profile shaping approach not only offers a new detection mechanism for single molecules, but also has excellent potential for studying protein interactions and the intracellular detection of mRNA.

1. Introduction

The concept of the "nanoruler", which entails the measurement of nanoscale distances based on the spectral peak shift due to localized surface plasmon resonance (LSPR) coupling between two gold nanoparticles, suggests a new paradigm of spatial scaling in biology beyond the optical resolution afforded by nonfluorescent methods.[1–3] Under appropriate conditions, this concept can be applied to study physical[4,5] and biological[6,7] systems as a complementary approach to fluorescence resonance energy transfer (FRET). Although the LSPR peak shift study comprising plasmon resonance energy transfer (PRET)[8] is an established technique for single-molecule studies, multiplexing is cumbersome. However, when using Raman scattering, a well-known technique for biomolecule profiling and multiplex detection,[9] the detection of single molecules with information on interaction distances between molecules can be achieved in a multiplex format.

Large enhancement for measurable surface-enhanced Raman scattering (SERS) signaling is possible from geometric

Dr. K. Lee, Prof. J. Irudayaraj
Department of Agricultural and Biological Engineering
Bindley Biosciences Center
Birck Nanotechnology Center,
and Purdue Center for Cancer Research
Purdue University
225 South University Street, West Lafayette, IN 47907, USA
E-mail: josephi@purdue.edu

DOI: 10.1002/smll.201201985

NANO MICRO small

configurations of nanostructure, such as tapered structures, gaps, or random aggregates. Past efforts have shown that the peaks in a single Raman spectrum of a dye molecule are enhanced differently (termed "SERS profile shaping" or "SERS shaping") and are dependent on the laser excitation wavelengths[10] or the LSPR peaks of the enhancer.[11–14] However, a complete and systematic study to extract LSPR information from the SERS signal has not been reported. For example, near-field profiling by Raman[15] and fluorescence[16] spectroscopy has been performed, but the signal intensity variation due to instrumental effects has been ignored; hence, detecting single molecules has been a challenge. Recently, the conceptual proof of Raman shaping due to the plasmon effect from single molecules has been investigated.[17] However, the Raman signal from a single molecule elicits signal fluctuation, especially when single-molecule binding is not regulated. When this effect is accompanied by structural deformation of the targets, severe signal variation can be noted.[18] Thus, LSPR signal extraction from SERS data has always been a challenge.

In this research, we standardized and derived a one-to-one correspondence between LSPR and SERS shaping by considering a step-by-step process of signal shaping. We demonstrate that the Raman nanoruler approach may be used for quantification and distance measurements at the single-molecule level. By choosing appropriate resonant labels, we show that multiplexing is also possible.

2. Results and Discussion

A one-to-one correspondence between LSPR and SERS has not been clearly formulated at the single-molecule level for several reasons (**Figure 1**a). First, there must be a nonresonant SERS signal measurement as a good reference to extract the LSPR signal from resonant or preresonant SERS data. Because the Raman signal of dye molecules cannot be directly compared with the SERS signal due to the peak position change by the SERS selection rule,[19,20] the reference signal should also be a SERS signal from the same nanoparticles but without the LSPR configuration. Second, the SERS signal should be stable and repeatable, without signal fluctuation or blinking. However, if signals from several dye molecules are averaged, an average consistent SERS signal could be obtained and signal fluctuation due to SERS blinking may be eliminated.[21,22] More importantly, the nanoparticle configuration should not change during measurement, such that consistent LSPR signals can be obtained from structures that are rigid and from single-molecule targets.[18] Third, signal enhancement from nanoparticle dimers cannot be clearly differentiated from signals consisting of a small fraction of nonspecifically aggregated particles. To overcome this hurdle, hetero dimers have been proposed to confirm the dimerization,[23,24] but this approach generated drastic spectral broadening, which resulted in an ambiguous configuration due to the different material properties. The original signals were thought to be deformed as a result of the instrumentation optics and measurement.[25,26]

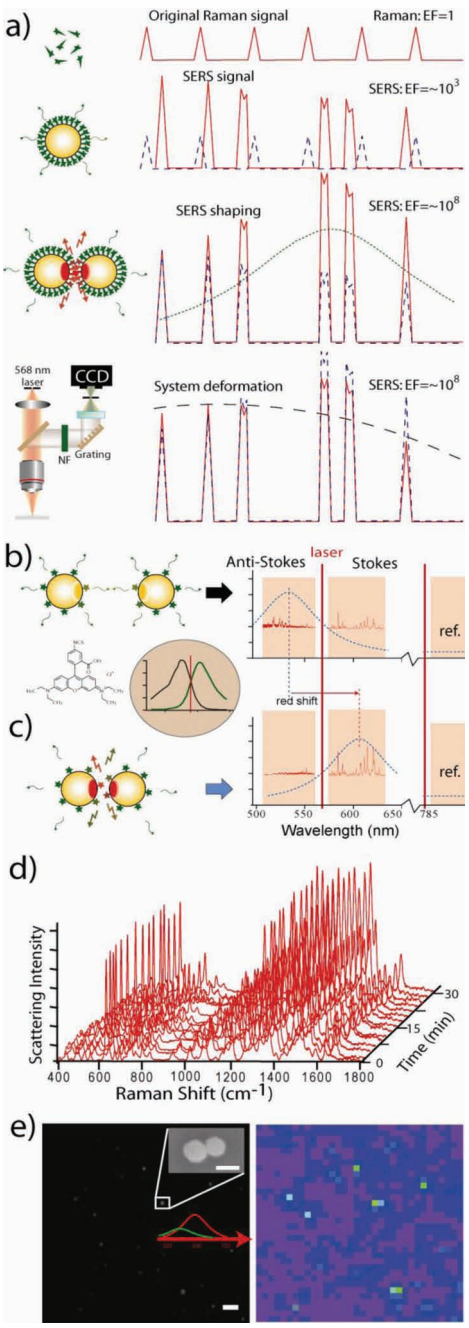

Figure 1. Schematic of the SERS nanoruler concept, showing distance-dependent enhancement of the Raman-labeled (star symbol) functionalized gold nanoparticles. a) Particles separated by a larger distance show a low average enhancement factor (EF), with maximum enhancement at 538 nm (anti-Stokes range of 568 nm excitation). b) As the interparticle spacing decreases, the LSPR peak red-shifts to a position in close proximity to the Raman measurement wavelength range (right side of the laser excitation line), which results in a high average enhancement, with a maximum at 612 nm. c) Signal deformation depended on the sample preparation and instrumentation. d) The SERS spectrum of rhodamine B isothiocyanate (RBITC)-modified nanoparticle dimer, the axis of which was parallel to laser polarization, obtained under continuous illumination for over 30 min shows no blinking. e) Dark-field image with white illumination and SERS image corresponding to the 1648 cm^{-1} SERS peak. Inset: SEM image and LSPR spectrum (red) of typical nanoparticle dimer and spectrum of monomer (green) as a reference.

Hence, if the excitation wavelength or the instrument is changed, the whole spectral profile changes, even though the peak positions are the same. This outcome is due to the differences in the sensitivities of the CCD camera and optical components in the light path, which distort the Raman profile even without any plasmon enhancement. This type of signal deformation causes a disparity in SERS-shaping studies by plasmon resonance and has not been addressed in previous studies. To our knowledge, our study is the first to successfully extract the full LSPR profile from SERS measurements to confirm the LSPR peak position for single-molecule detection, although SERS shaping by LSPR has been reported abstractly. Hence, it is necessary to study the one-to-one correspondence between the LSPR profile and the SERS measurement of the single nanoparticle dimer in this formulation.

The one-to-one correspondence between LSPR and SERS shaping was demonstrated by considering the following concepts. First, we normalized the SERS signal from the dimer by either the SERS signal of the monomer at high concentration, or by the SERS signal of single dimers excited by laser with a wavelength that was far longer than the LSPR resonance. The peak positions of both reference SERS signals were similar to that of the SERS signal, which included the LSPR information, measured from the dimers. Information on the SERS-shaping profile could be obtained upon normalization of the signal by the reference.

Second, we addressed the signal fluctuation from single molecules by considering two key aspects: signal blinking, which is minimized by optimizing the number of Raman labels on the probe, and stability of the nanoparticle geometry, which is regulated by the construction of well-defined structures with interparticle distances by using hybridized double-stranded DNA (dsDNA) molecules of different sequence lengths. Nanoparticle dimers composed of dsDNA linking two nanoparticles are robust enough to withstand the attractive optical forces of several pico-Newtons between nanoparticles[27] and maintain a constant interparticle distance.[4,28–30]

Third, we used the bianalyte method, in which nanoparticles for different targets were labeled with distinct dye molecules, to ensure that the signal was from specific dimers instead of nonspecific aggregates. Because the SERS signal is predominantly from hot spots between two nanoparticles, the signal from the two different Raman labels is clear evidence of specific structures with this configuration. Other considerations constituting signal deformation by the instrument were addressed, and calibrations were performed according to the National Institute of Standards and Technology (NIST) protocol[31] to minimize signal variability due to optical components.[25,26]

Herein, we demonstrate a SERS-based scaling concept as a sensitive nanoruler for single-molecule detection in biology for quantification, multiplex detection, and structural analysis. Figure 1b and c describe a representative experimental design to optimize the conditions for SERS-shaping experiments. Gold nanoparticles were used as SERS substrates, because they are stable, monodispersed, and biocompatible. Specific and intense Raman signals were obtained from the SERS experiments, which were performed with rhodamine B isothiocyanate (RBITC) excited by a 568 nm laser to maintain resonant Raman conditions. Gold nanoparticle probes (40 nm in diameter) were designed to differentiate clearly between monomers and dimers, on the basis of the LSPR peaks observed in the anti-Stokes and Stokes regions, respectively.[32] Gold nanoparticle monomers have an LSPR peak at ≈540 nm and dimers have a peak at ≈600 nm when the interparticle distance between two nanoparticles is approximately 2 nm. This range is also relevant for SERS, because it covers the range between 574 and 633 nm in the Stokes region, and from 515 to 560 nm in the anti-Stokes region. A 568 nm laser excitation was selected for three important reasons: 1) the chosen dye RBITC can generate a resonant Raman signal at this excitation wavelength; 2) major anti-Stokes and Stokes Raman signal ranges include LSPR peaks of monomers and dimers, respectively; and 3) the excitation wavelength can induce significant enhancement and avoids interband excitation of gold atoms. By using the proposed design, the maximum intensity of the Raman signal was obtained without blinking, to demonstrate the SERS-based signal shaping due to the LSPR peak shift.

Raman spectra were obtained at their maximum intensity due to parallel polarization under continuous illumination for over 30 min (Figure 1d). It was possible to obtain consistent spectra, because the signal was obtained from multiple dye molecules functionalized onto the surface of the nanoparticles with minimum blinking effects. A stable signal implies constant enhancement, thus affirming that dimers formed from DNA hybridization offer a stable interparticle distance that can overcome the steric hindrance of large nanoparticles. In this work, we will show that the proposed particle design can be used as an effective sensing tool, by using antibody–antigen constructs as an example.

The measured Raman signal covered the range between 574 and 633 nm in the Stokes region and between 515 and 560 nm in the anti-Stokes region. Hence, measurement of both anti-Stokes and Stokes Raman signals will clearly span the whole range of LSPR peaks (500–650 nm) of nanoparticle dimers formed with various interparticle distances. Our probe synthesis resulted in the attachment of approximately 800 RBITC molecules on the surface of a single nanoparticle (Supporting Information, Table S2). Figure 1e shows the dark-field image and SERS hyperspectral image with respect to the SERS peak at 1648 cm^{-1}, which indicate that SERS signals from the nanoparticle dimer were due to hot spots between nanoparticles. The SERS signal was detected only on spots of the dark-field image, showing an LSPR peak at 614 nm (Figure 1e, inset) of the dimer, with an interparticle distance of <2 nm in the scanning electron microscopy (SEM) image (inset).

The one-to-one correspondence between SERS profile shaping and LSPR was demonstrated in the cross-platform measurements of SERS and LSPR signals from nanoparticle dimers by using polarized excitation, thus implying a similar functional and phenomenological relationship between SERS and LSPR. Both the LSPR and Raman signals were measured by changing the polarization of light with a polarizer and a $\lambda/2$ waveplate. In **Figure 2**a, the calculated LSPR peak and the experimental results are shown together with the calculated Raman intensity, along with the experimental

small NANO MICRO

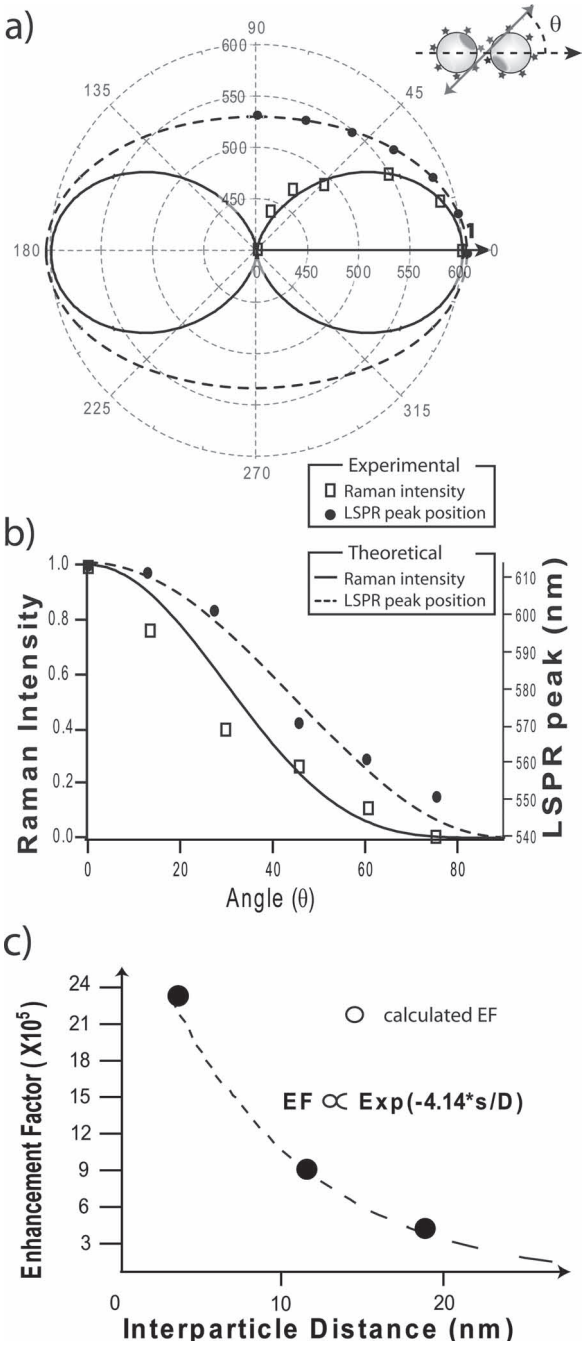

Figure 2. a) Polarization dependency of both LSPR peak position and SERS signal intensity expressed in polar coordinates. The radial axis represents the LSPR peak position in dark-field measurements or normalized Raman signal intensity in SERS measurements; the angular axis represents the polarization angle between the polarized light and the dimer longitudinal axis (inset). Both theoretical (lines) and experimental results (dots) are shown. b) LSPR peak measurements based on the polarization of dimers distributed on a glass slide fitted with the functions of ($\lambda_{max}\cos^2\theta + \lambda_{min}\sin^2\theta$) and $\cos^4\theta$, respectively. c) Enhancement factor (EF) calculated from dimers with different interparticle distances. Enhancements of dimers with large interparticle distances (12.5 and 23 nm) were from highly concentrated (pM to nM) samples.

readouts. An example of an LSPR measurement with polarization change is presented in the Supporting Information (Figure S4).

Interestingly, in the LSPR range considered (≈536 nm for perpendicular polarization and >600 nm for parallel polarization), most of the LSPR peak values fell around the maximum (40%) and minimum (40%) LSPR range, and 20% of the values fell in the middle bandwidth (565–590 nm) of the LSPR range, depending upon the polarization condition (Figure 2b). Our calculations suggest that these measurements are likely to be close to either the maximum (peak position) representing the dimer or the minimum representing the monomer when measured at random polarization (orientation).

The measured LSPR peaks that are contained in the regions comprise bands in the range from 590 to 615 nm and from 540 to 565 nm, as shown in Figure 2b. In these measurements, the normalized Raman intensity of the characteristic signature of the RBITC label at 1648 cm^{-1} was considered for the polarization condition with 568 nm laser excitation. The results showed that the distribution of SERS enhancement (Figure 2b) was similar to the LSPR peak distribution with respect to the maximum or minimum value, depicting a parallel or perpendicular polarization condition, respectively. As expected, it was not possible to measure the Raman signal for the minimum enhancement (≈10^3) condition. Among other factors, including the LSPR condition, the interparticle distance plays a critical role in SERS enhancement.[33] In terms of dimers, the interparticle distance could be directly related to the LSPR condition for a given particle size.[1] Such a system allows us to assess the maximum LSPR peak position that corresponds to an interparticle distance when the laser polarization is parallel to the dimer axis after the statistical analysis of multiple measurements, due to SERS signal shaping. Thus, from SERS shaping and multiple measurements of dimers under different polarization states, the maximum LSPR peak position can be determined and the corresponding interparticle distance can be calculated.

SERS enhancement can be determined by the highest local field intensity from hot spots. The enhancement factor, which depends on the polarization, was calculated on the basis of the intensity of the Raman signal, to enumerate the effect of polarization on the enhanced Raman signal.[34] In the dimer approach, hot spots were expected to occur at the interspace between gold nanoparticles, as shown in Figure 2c. The enhancement factor may serve as an excellent indicator of the distance between nanoparticles in a dimer. It was not possible to obtain a SERS signal from a single nanoparticle dimer when the interparticle distance was larger than a few nanometers (>4 nm) because of the apparent low enhancement.[35] Therefore, when the interparticle distance was increased (for example, >4 nm), a higher concentration of dimers could be used, and the $\cos^2$ signal may be employed to evaluate the interparticle distance of individual dimers, as introduced in former research.[36] By varying the concentration of dimers, the enhancement factors were calculated for each of the dimers constructed, and the interparticle distance was directly evaluated from the intensity.

The resulting enhancement factor was fitted with an exponential function, which was proportional to a factor of $\exp(-4.14 \times s/D)$ and agreed well with other studies.[5] The relationship between enhancement and LSPR shift from

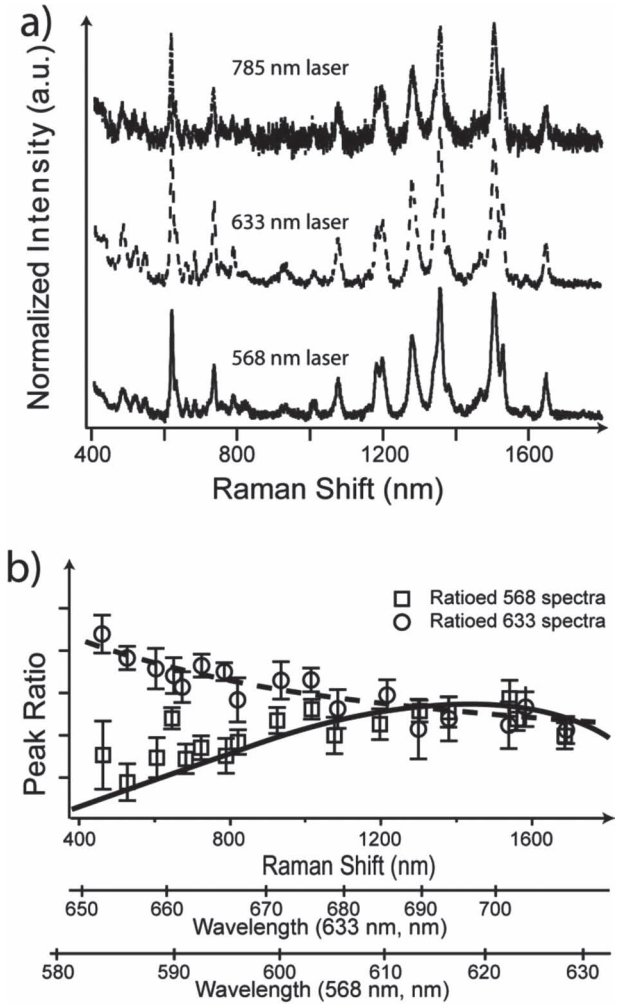

Figure 3. SERS profile shaping under different wavelength excitations. a) Corrected Raman signals from RBITC-modified gold nanoparticle dimers with an LSPR peak of 613 nm obtained with 568, 633, or 785 nm laser excitation. b) Spectra from 568 and 633 nm excitations, normalized with the 785 nm excitation (nonresonant or least resonant condition) as a reference. Raman shaping shows information about the plasmon resonance.

nanoparticle dimers is depicted in Figure 2b. The highest enhancement was obtained when the LSPR shift was at its maximum (for an interparticle distance <2 nm). Raman enhancement is more sensitive to polarization because of its $|E|^4$ dependence, whereas LSPR has an $|E|^2$ dependence. Although the Raman enhancement factor can be fitted by a $\cos^4$ function, LSPR is fitted by the $(\lambda_{max}\cos^2\theta + \lambda_{min}\sin^2\theta)$ function. We will show that both the SERS shaping and the enhancement factor evaluated from dimers are excellent indicators of LSPR peak position and of interparticle distance.

Figure 3 shows that the LSPR signal could be successfully extracted from the SERS signal by calibration and normalization. A one-to-one correspondence can be observed by examining Figure 2a and b, in which their interdependence and functionality are shown to be analogous. Here, the average intensity of each peak was obtained from several measurements (on average, three to five measurements) to reduce the possible fluctuation or minor blinking effects arising from signals obtained from a small number of molecules in the hot spot, or a change in orientation of the molecules relative to the surface of the nanoparticles.[20,37]

In our experiment, SERS signals from dimers with the shortest interparticle distance were obtained for three different laser excitations, 568, 633, and 785 nm, with polarization parallel to the axis of the dimer, to assess the dependency of SERS profile shaping on the excitation wavelength. As expected, different SERS profile shapes were observed for different excitation wavelengths (Figure 3a), corresponding to the respective interparticle distances. Therefore, the LSPR response of the nanoparticle dimers could be obtained from SERS profile shaping, which agreed well with our designed nanoparticle dimers.

Next, we demonstrated that the number of dimers could be quantified with both LSPR and SERS by statistical analysis, which will overcome the signal variation due to the possible floppy nature of the thiol–nanoparticle junction. All measurements were performed by using dimers of different concentrations that were randomly distributed on polylysine-coated glass slides. An increase in the proportion of dimers compared to monomers was noted, which corresponded to an increase in the concentration (from 5 to 100 pM) of the target sequence (ts1), as illustrated in **Figure 4**a. The number

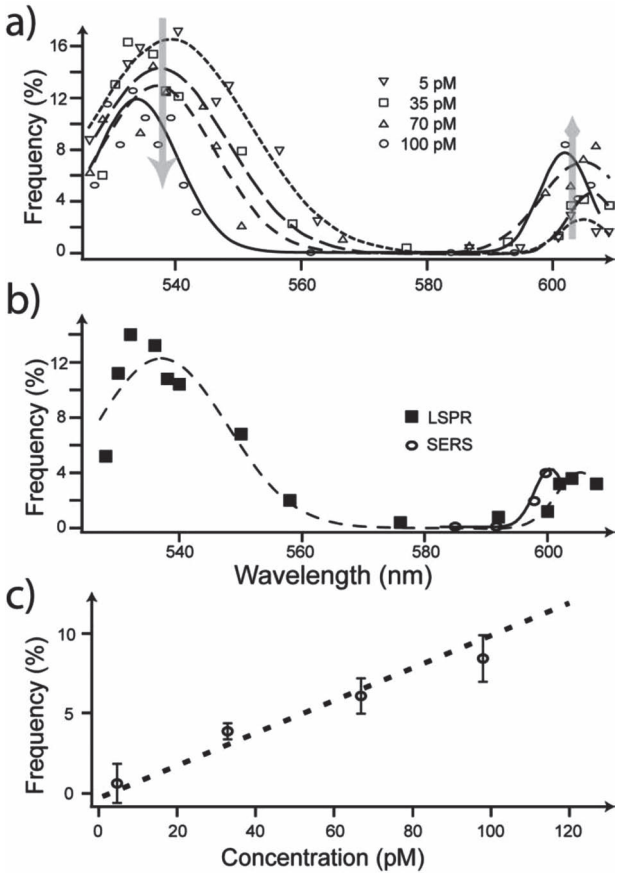

Figure 4. Quantification of nanoparticle dimers by both LSPR and SERS measurements. a) LSPR quantification of dimers with respect to the concentration of the target sequence. b) Comparison of SERS-based and LSPR-based dimer quantification. c) Calibration curve for quantification with a linear fit by SERS shaping.

NANO MICRO small

of samples in the monomer wavelength range (≈540 nm) decreased, whereas the number in the dimer wavelength range (≈605 nm) increased.

In Figure 4b, a similar trend was observed from the measurements by LSPR and SERS, with a ts1 concentration of 35 pM. Data for monomers could not be obtained by SERS because of the low enhancement when the samples were present in monomer form or when dimers were examined under a perpendicular polarization condition. Also, the SERS-shaping peak distribution over the polarization angle formed peaks that were sharper than those with the LSPR, because SERS shaping has a $\cos^4$ dependency with respect to polarization, which is more sensitive than the $\cos^2$ dependency, as depicted in Figure 2. Because the contribution of parallel polarization is more pronounced in SERS shaping, this condition presents the most consistent information (smaller standard deviation) when excited with a polarized light source.

Figure 4c shows that the calibration for concentration followed a linear trend, thus confirming the fact that the SERS signal shaping occurred due to the plasmon coupling in a dimer configuration. Compared to the conventional SERS intensity-based quantification by Poisson fitting, the quantification of dimers by the proposed SERS shaping analysis was 2.5-fold greater.[38] This result is reasonable, because statistical SERS shaping-based quantification includes information from dimers with random polarization, whereas the intensity-based analysis by Poisson distribution does not account for these variations.

The nanoruler profile over a wide range of wavelengths was also demonstrated from the Stokes and anti-Stokes measurements. A clear difference in signals was observed between nanoparticle dimers that were spaced within 2 and 18 nm in the Stokes and anti-Stokes regions, respectively (**Figure 5**a and b). Again, even though the Raman peak position, that is, Raman shift read, was the same, the signal intensity profiles in Figure 5a and b were different (gray arrows). When the signals were normalized with respect to the reference SERS signal measured by the 785 nm excitation (in the nonresonant condition), the difference was more pronounced in the extracted LSPR profiles (Figure 5c). Because the anti-Stokes signal had a very low signal-to-noise ratio at the 785 nm excitation, the Stokes signal was used as a reference. By employing both Stokes and anti-Stokes SERS measurements, a wide range of SERS signal measurements (150–200 nm window in this experiment), together with SERS shaping, were possible.

We applied the developed SERS nanoruler concepts to detect and measure the distance between two binding entities by using immunoglobulin G (IgG) fragments. The interaction between the modified Fc and Fab binding sites is demonstrated in **Figure 6**a and b, whereas the interaction between Fab and Fab using SERS shaping is shown in Figure 6c and d. Different Raman labels denote the presence of the respective modifications. In these measurements, the SERS signal of Raman-labeled gold nanoparticle monomers (≈5 nM), excited by the 785 nm laser, was used as the reference.

The conceptual design and the Raman signal measured from bianalyte nanoparticle dimers are shown in Figure 6a

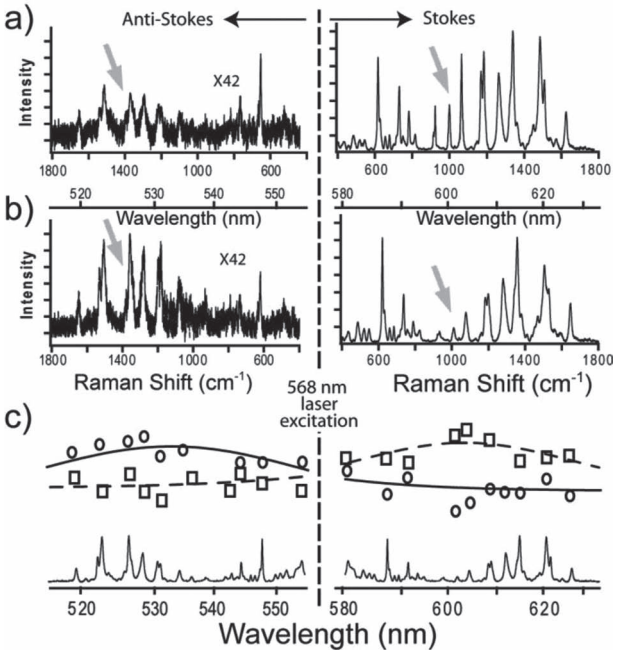

Figure 5. Anti-Stokes and Stokes spectra of RBITC-modified nanoparticle a) head–head dimers and b) tail–tail dimers from hybridization of 68 base pair (bp) complementary DNA. Stokes measurement clearly shows the enhancement of the head–head dimers (a, right) and not the tail–tail dimers (a, left). Enhancement of tail–tail dimers is seen in the anti-Stokes (b, left) and not in the Stokes (b, right) region. c) SERS shaping of head–head dimers (dots) in the Stokes and tail–tail dimers (line) in the anti-Stokes region. Bottom: SERS reference signal (green) of monomers for both anti-Stokes and Stokes regions, excited by 785 nm laser.

(Fc and Fab) and 6c (Fab and Fab), respectively. In Figure 6b and d, the two dye molecules representing the modifications showed the SERS profile shaping, which occurred at almost the same peak positions. In other words, both RBITC and crystal violet (CV) for Fc and Fab showed the SERS-shaping peaks at 610 nm (Figure 6b), whereas both RBITC and malachite green isothiocyanate (MGITC), representing Fab and Fab, respectively, showed the SERS-shaping peaks at 612 nm (Figure 6d). Thus, these results are in agreement with each other. These findings are supported by the structure of IgG because Fab and Fc are of similar size, with almost the same angle between them.[39]

The SERS-shaping pattern of the two different dye molecules at the same wavelength is a good indicator of signals originating from hot spots enhanced due to the strong LSPR signals originating from hot spots from dimers. This fact excludes the possibility that signals are from uncontrolled aggregation. It is also confirmed by the fact that neither the RBITC–RBITC nor the CV–MGITC SERS shaping could be detected, as expected due to the design. Indeed, the bianalyte signal of CV–RBITC could not be observed from papain-treated samples, nor could the MGITC–RBITC signal be observed from pepsin-treated samples (data not shown). These findings support the notion that these signals are from Fab–Fab and Fc–Fab, respectively. This simple demonstration shows that the SERS profile shaping can be used to study the

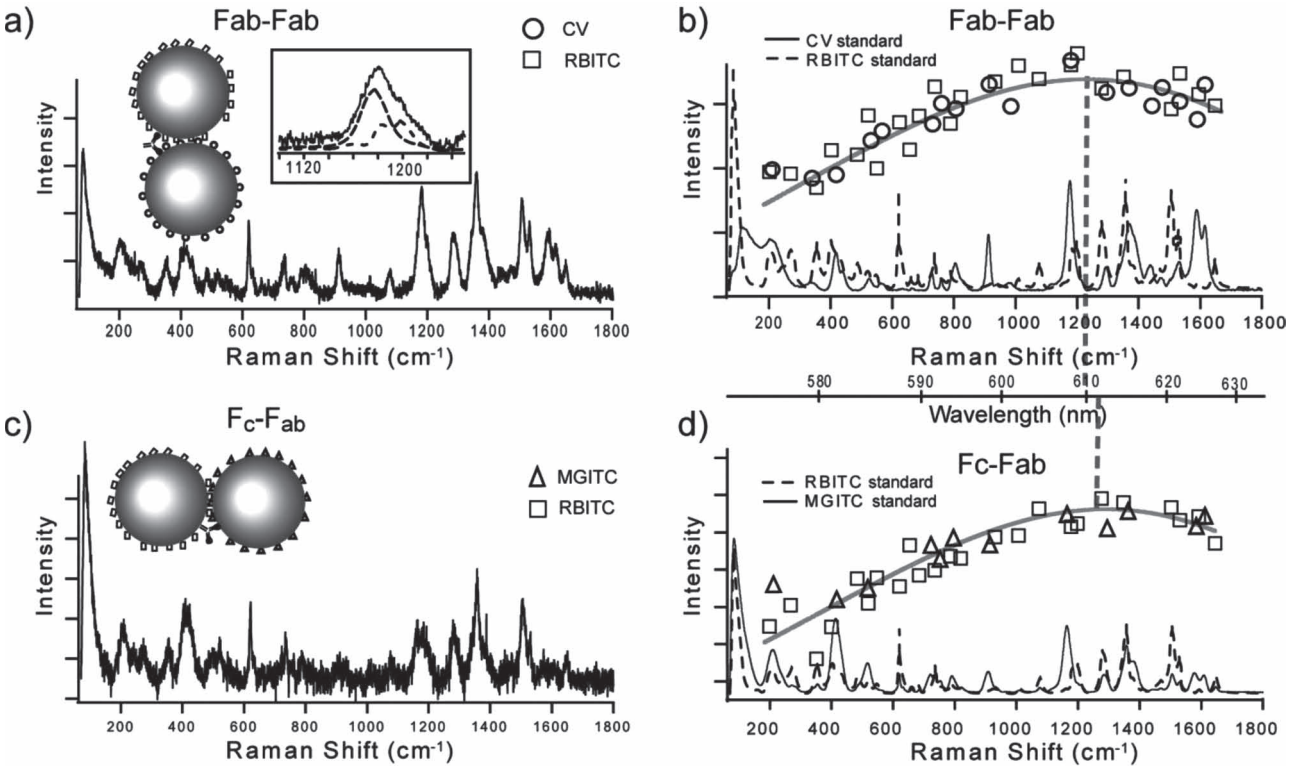

Figure 6. a) SERS signal from nanoparticles targeting Fab and c) Fab and Fc. b,d) SERS profile shaping and characteristic peaks of each dye molecule in (a) and (c), respectively. The peaks of SERS shaping agree with the LSPR peaks. a) Inset: example of a SERS-shaping factor calculated by Gaussian fitting of the measured signal with two reference SERS signals of the respective molecules excited by 785 nm laser.

structural analysis of single biomolecules and to reveal their colocalization at a high resolution.

3. Conclusion

In summary, the LSPR profile was extracted from the SERS signal for interparticle distance measurement and quantification with multiplexing. We have demonstrated a clear one-to-one correspondence between LSPR and SERS shaping with respect to the plasmonic peak position, per the NIST standard. In addition, we revealed the interparticle distance from the extracted LSPR profile to validate the SERS nanoruler concept for the first time. Importantly, our approach has the advantage of clearly differentiating dimers from nonspecific aggregation in the bianalyte signals. Future work may include the application of our method to various purified intracellular/intranuclear proteins, to verify their structural geometry under different modifications, for example, histone modifications in a nucleosome for epigenetic profiling.

Experimental Section

Reagents: Ultrapure water (18 MΩ cm^{-1}) was used throughout the experiments. Dye molecules, including rhodamine B isothiocyanate (RBITC), crystal violet (CV), and 4-mercaptopyridine (4-MPy), were purchased from Sigma, and malachite green isothiocyanate (MGITC) was from Invitrogen. Oligonucleotides with the following sequences (Supporting Information, Figure S1 and Table S1) were purchased from IDT:

Probing sequence 1 (ps1): 5′-GCT GCT TGT GAA TTT TCT GAT TTT TTT TTT/3ThioMC3-D/-3′

Target sequence 1 (ts1): 5′-TCA GAA AAT TCA CAA GCA GCC AAT TCA ATG TAG ACA GAC G-3′

Probing sequence 2 (ps2): 5′-/5ThioMC6-D/TTT TTT TTT TCG TCT GTC TAC ATT GAA TTG-3′

Target sequence 2 (ts2): 5′-CAA TTC AAT GTA GAC AGA CGT CAG AAA ATT CAC AAG CAG C-3′

Complementary sequence-1 (cs1): 5′/5-Thiol MC6-D/TTT TTT TTT ACT TGG CGG AT-3

Complementary sequence-2 (cs2): 5′/5-Thiol MC6-D/TTT TTT TTA TCC GCC AAG TA-3

Protecting sequence: 5′/5-ATG CAA ACA GCT TTT TTT TTT T/3-Thiol MC3-D/3′

Thiol-PEG-CH_3O and thiol-C_2H_4-CONH-PEG-C_3H_6-COOH were purchased from Rapp Polymere (Germany). Coverslips with a photoetched grid for nanoparticle tracking were obtained from Belco Glass. Phosphate-buffered saline (PBS), cell culture media, fetal bovine serum, and cell culture supplies were purchased from the American Type Culture collection (ATCC). *N*-Ethyl-*N*′-[3-(dimethylamino)propyl]carbodiimide (EDC) and *N*-hydroxysuccinimide (NHS) were purchased from Thermo Scientific. All other reagents were obtained from Sigma–Aldrich at the highest level of purity.

Preparation of Nanoparticle Dimer: Raman-labeled and DNA-modified gold nanoparticles were constructed by hybridizing complementary single-stranded DNA (ssDNA),[40–42] as shown

NANO MICRO small

in our previous study,[32,43] with minor modifications. Roughly, head–head dimers were prepared by adding ts1 sequences to a mixture of ps1- and ps2-modified gold nanoparticles. Similarly, tail–tail dimers were prepared by adding ts2 sequences to the probe nanoparticles mixture. Other dimers with a medium interparticle distance (≈12 nm) were prepared by hybridizing cs1- and cs2-modified probe nanoparticles. To ensure the formation of single dimers, nanoparticles were modified with a desired number of probe DNA strands (i.e., PS sequences) and protecting DNAs to ensure stability. The nanoparticles were estimated to contain approximately 1–2 PS strands per particle and hundreds of protecting DNAs to ensure the stability[44,45] of the dimer structures. Details are described in the Supporting Information. Buffer condition (1X PBS, pH 7.4, room temperature) was strictly maintained to ensure the formation of consistent DNA structures.

Preparation of Immunoglobulin Antibody Nanoprobes: Nanoparticle probes modified with anti-Fc and anti-Fab antibodies and Raman dye molecules were prepared.[46] Briefly, a fresh solution with a dye concentration of 3 μM was added dropwise to the gold nanoparticle solution to result in a 1 μM final concentration, and mixed rapidly to guarantee a uniform reaction. After 10 min, HS-PEG-COOH solution (200 μL, 1 μM) was added to the Raman-labeled nanoparticle solution (1 mL). After 30 min of incubation, thiol-PEG solution (0.5 mL, 10 μM) was added dropwise and rapidly mixed. After 30 min, the solution was centrifuged twice (1000 *g*, 12 min) and resuspended in PBS. To activate the -COOH group, fresh EDC (5 μL, 50 mg mL^{-1}) and NHS (5 μL, 100 mg mL^{-1}) were added to the solution and mixed vigorously at 4°C for 30 min. The solution was centrifuged twice (1000 *g*) and resuspended in PBS. Then, anti-IgG antibodies were added to the solution and stored at 4 °C overnight. Finally, the solution was centrifuged (1000 *g*, 15 min) and resuspended in PBS buffer for further experiments (Supporting Information).

Nanoprobe Characterization: UV/Vis spectra were obtained after the addition of solution and supernatants to estimate the number of molecules modified onto the single gold nanoparticles. Transmission electron microscopy (TEM; Philips CM100, FEI, Hillsboro, Oregon) and dynamic light scattering (DLS; Zetasizer Nano, Malvern Instruments Ltd., UK) were used to monitor and assess the number of molecules on nanoparticles. The DLS measurement also confirmed successful dimer formation without large aggregation (Supporting Information, Figure S2).

LSPR Peak Measurement: The LSPRS peak position of the nanoparticle dimers excited by a tungsten–halogen lamp (Illumination Technology, NY) filtered by a polarizer was measured with a cooled CCD camera (Princeton Instruments, PA) with a 40× air objective lens (numerical aperture, NA = 0.75, Olympus, Japan) and a home-built dark-field spectroscopy unit.[21]

Raman Measurement: The Raman signal from each of the nanoparticle dimers was measured with a 50× long working distance lens (NA = 0.9, Olympus, Japan), by using three different laser excitations (568, 633, and 785 nm) at 1–10 mW. The signal intensity was measured for an accumulation time of 10–150 s (T64000, Horiba & Senterra, Bruker Optics Inc.). To study SERS profile shaping, three Raman labels were selected, with characteristic peaks spanning over a wide range (400–1800 cm^{-1}) and an excitation frequency (568–785 nm) in the LSPR range of gold nanoparticles. All measurements were performed in buffer to avoid NaCl crystal formation. Control experiments, such as measurements of nanoparticle probes without Raman label (RBITC dye molecules) or without DNA modification, did not show any meaningful Raman signal (Supporting Information, Figure S3). Different combinations of dye molecules, laser wavelengths, and interparticle distances were selected to cover the resonance options (resonant, preresonant, and nonresonant) for a chosen Raman label corresponding to the LSPR response of the monomers and dimers. When the chosen label was excited by an optimal laser source, the signal-to-noise ratio was expected to be high because of the resonance, whereas excitation by other laser lines would produce an enhanced spectrum that may not be the maximum. However, as long as a detectable signal could be recorded, analysis was possible with appropriate calibration by using dimers of varying interparticle distances.

Polarization Dependency: Prepared gold nanoparticle dimers were placed on a coverslip modified with polylysine (1 mg mL^{-1}) for uniform distribution.[17] Both LSPR and Raman signals were measured after the formation of nanoparticle dimers on the coverslips. Measurements were performed with rotation of the sample by 15° by using a $\lambda/2$ waveplate.

Excitation Wavelength and Dye Molecules: Different laser wavelengths and dye molecules were used to study the effect of laser/dye selection on enhancement. Laser lines 568, 633, and 785 nm were selected to provide information on enhancements under conditions in which they are close to or further away from the LSPR peak of the nanoparticle structures. Three dye molecules, RBITC, CV, and 4-MPy, were chosen because of their affinity to the metal particles and high Raman cross section.

Interparticle Distances and Nanoparticle Size Ratio (s/D): Three different interparticle distances obtained by DNA hybridization were combined with two different nanoparticle sizes (25 and 40 nm). Head-to-head dimers in the sandwich structure yielded the closest interparticle distance (≈2–3 nm), thereby generating the strongest Raman signal due to high enhancement based on the strong plasmon coupling. DNA hybridizations of 28 and 60 bp offered two different interparticle distances; therefore, in total, six different ratios (s/D) could be obtained (Supporting Information, Figure S1).

Signal Corrections and SERS-Shaping Measurement: Raman signal intensity profiles from the same sample can be different when the excitations and optics have different configurations, even if their Raman shift positions are the same.[47] Hence, careful data calibration should be performed. While changing the laser wavelength, the Raman spectra of pure RBITC molecules with high concentration were measured, to determine the calibration factor for each system and to compensate for the effect of several factors involved in signal shaping, such as grating structures and materials, CCD sensitivity at different wavelengths, optical differences, and numerical aperture, to name a few, in the manner similar to that in the NIST standard.[25] All of the measured Raman signals were corrected relative to the spectra measured with the 785 nm source. Measured SERS signals were normalized after baseline correction and divided by the SERS signal obtained from the 785 nm excitation. Normalization with the signal measured by 785 nm excitation, which is far from the LSPR peak position of the nanoparticle structure, was chosen, because the reference signal should be free from SERS shaping.

In our design, all of the plasmon resonance peaks were in the wavelength range between 530 and 610 nm, and their full width

at half maximum was within 90 to 150 nm. Hence, Raman signals obtained with 785 nm excitation were used for reference, because this excitation provides a resonance-free condition (Figure 1a and b). All SERS-shaping profiles in the subsequent analyses were obtained after normalization by the 785 nm SERS signals.

Quantification: Quantification of head-to-head dimers among the unbound single nanoparticles was first demonstrated. Head-to-head dimers in the sandwich structure generated the most distinguishable signals, because their proximity yielded the smallest interparticle spacing. The number of dimers present could be controlled by incubating the PS ssDNA-bearing particles with different concentrations of target sequences that would complement the probe sequences 1 and 2 to form the dimer structure. After dimer formation in solution, 20 μL of 30 pM solution was identified on a polylysine-coated glass slide, and the substrate was washed after 30 min to ensure a moist condition and to prevent the formation of salt crystals. Both the LSPR and SERS signals were measured. Poisson fitting of statistical data was performed to provide information on the dimer concentration.

Stokes and Anti-Stokes SERS-Shaping Measurement: Dimers with different interparticle distances (≈2 and ≈18 nm formed by head-to-head and tail-to-tail dimers from the same batch used in other experiments) excited by 568 nm laser were used to illustrate this concept. When the dimer was excited by a 568 nm laser, both Stokes and anti-Stokes signals were collected. The 568 nm laser excitation was selected to cover both the weak (≈540 nm, anti-Stokes) and the strong (≈610 nm, Stokes) LSPR peaks. Gold nanoparticle dimers with larger interparticle distances, formed by the hybridization of complementary ssDNA consisting of 60 bp (40 bp complementary sequence + 2 × 10 bp linker sequence of each probe), that is, ≈18 nm in length, were also tested to confirm that SERS shaping could be observed at higher concentrations.

Because the enhancement of nanoparticles with larger interparticle distances was not sufficient to generate a measurable signal from dimers (Figure 2c), highly concentrated samples (≈4 nM) were used for Raman measurements. In this case, the polarization of nanoparticle dimers was not controlled and measurements were performed under the random condition to show the SERS-shaping effect. However, because the dominating SERS signals were from hot spots between nanoparticle dimers, a certain difference in measurement between samples with different interparticle distances (≈2 nm due to a head-to-head dimer, and 20 nm from hybridization of 60 bp sequences) was expected, as shown in Figure 5b. The SERS profile shaping was not as significant for single dimers with a larger (>4 nm) interparticle distance compared to that with a smaller spacing, because the enhancement was not sufficient. Furthermore, a significant number of monomers were present in the sample. Thus, for reliable detection, sufficient signal enhancement was necessary to observe a clear SERS profile shaping from a population with a high concentration of dimers with larger interparticle distances. From our experiments and testing conditions, a nanomolar concentration of dimers with ≈10 nm spacing revealed detectable signals by SERS shaping.

IgG Antibody Detection: Nanoparticles modified with respective anti-Fc (BS3) and anti-Fab antibodies were used to target different sites of IgG, Fc, and Fab. RBITC, CV, or MGITC were modified onto the nanoparticle probes to denote Fab, Fc, and the other Fab, respectively. Reagents with IgG were prepared in PBS buffer to ensure stability. First, one sample of IgG was incubated with 60 nm nanoparticle probes bearing RBITC and anti-Fab and nanoprobes bearing CV and anti-Fc for 4 h at 4 °C. The other sample of IgG was incubated with nanoprobes bearing RBITC and anti-Fab and nanoprobes bearing MGITC and anti-Fab for 4 h at 4 °C. Control experiments constituted nanoparticle probes without antibody, Raman dye, gold particles, or IgG. All samples were incubated on polylysine-coated glass slides for 30 min for uniform distribution.

Supporting Information

Supporting Information is available from the Wiley Online Library or from the author.

Acknowledgements

Funding for this work was provided by the NSF 0945771 award and the Purdue Center for Cancer Research Innovative award and a CTSI grant.

[1] K. H. Su, Q. H. Wei, X. Zhang, J. J. Mock, D. R. Smith, S. Schultz, *Nano Lett.* **2003**, *3*, 1087.
[2] C. Sonnichsen, B. M. Reinhard, J. Liphardt, A. P. Alivisatos, *Nat. Biotechnol.* **2005**, *23*, 741.
[3] R. F. Service, *Science* **2005**, *308*, 1099a.
[4] B. M. Reinhard, M. Siu, H. Agarwal, A. P. Alivisatos, J. Liphardt, *Nano Lett.* **2005**, *5*, 2246.
[5] P. K. Jain, W. Huang, M. A. El-Sayed, *Nano Lett.* **2007**, *7*, 2080.
[6] G. Rong, H. Wang, L. R. Skewis, B. M. Reinhard, *Nano Lett.* **2008**, *8*, 3386.
[7] L. J. Heon, P. W. Daryl, V. Y. Mehmet, L. Juewen, W. Zidong, L. Yi, *Angew. Chem. Int. Ed.* **2007**, *46*, 9006.
[8] Y. Choi, Y. Park, T. Kang, L. P. Lee, *Nat. Nanotechnol.* **2009**, *4*, 742.
[9] D. Graham, B. J. Mallinder, D. Whitcombe, N. D. Watson, W. E. Smith, *Anal. Chem.* **2002**, *74*, 1069.
[10] A. D. McFarland, M. A. Young, J. A. Dieringer, R. P. Van Duyne, *J. Phys. Chem. B* **2005**, *109*, 11279.
[11] X. Qian, J. Li, S. Nie, *J. Am. Chem. Soc.* **2009**, *131*, 7540.
[12] D. Graham, D. G. Thompson, W. E. Smith, K. Faulds, *Nat. Nanotechnol.* **2008**, *3*, 548.
[13] T. Itoh, K. Yoshida, V. Biju, Y. Kikkawa, M. Ishikawa, Y. Ozaki, *Phys. Rev. B: Condens. Matter Mater. Phys.* **2007**, *76*, 085405.
[14] T. Itoh, K. Hashimoto, A. Ikehata, Y. Ozaki, *Chem. Phys. Lett.* **2004**, *389*, 225.
[15] S. Lal, N. K. Grady, G. P. Goodrich, N. J. Halas, *Nano Lett.* **2006**, *6*, 2338.
[16] M. Ringler, A. Schwemer, M. Wunderlich, A. Nichtl, A. Kurzinger, K. Klar, T. A. Feldmann, *J. Physical Review Letters* **2008**, *100*, 203002.
[17] T. Dadosh, J. Sperling, G. W. Bryant, R. Breslow, T. Shegai, M. Dyshel, G. Haran, I. Bar-Joseph, *ACS Nano* **2009**, *3*, 1988.
[18] M. Ringler, T. A. Klar, A. Schwemer, A. S. Susha, J. Stehr, G. Raschke, S. Funk, M. Borowski, A. Nichtl, K. Kurzinger, R. T. Phillips, J. Feldmann, *Nano Letters* **2007**, *7*, 2753.
[19] S. H. Cho, H. S. Han, D.-J. Jang, K. Kim, M. S. Kim, *J. Phys. Chem.* **2002**, *99*, 10594.
[20] M. Moskovits, *Rev. Mod. Phys.* **1985**, *57*, 783.
[21] K. Lee, V. P. Drachev, J. Irudayaraj, *ACS Nano* **2011**, *5*, 2109.
[22] A. M. Michaels, M. Nirmal, L. E. Brus, *J. Am. Chem. Soc.* **1999**, *121*, 9932.
[23] S. Sheikholeslami, Y.-W. Jun, P. K. Jain, A. P. Alivisatos, *Nano Lett.* **2010**, *10*, 2655.

[24] L. V. Brown, H. Sobhani, J. B. Lassiter, P. Nordlander, N. J. Halas, *ACS Nano* **2010**, *4*, 819.
[25] P. C. DeRose, M. V. Smith, K. D. Mielenz, D. H. Blackburn, G. W. Kramer, *J. Lumin.* **2009**, *129*, 349.
[26] P. C. DeRose, M. V. Smith, K. D. Mielenz, D. H. Blackburn, G. W. Kramer, *J. Lumin.* **2008**, *128*, 257.
[27] A. J. Hallock, P. L. Redmond, L. E. Brus, *Proc. Natl. Acad. Sci. USA* **2005**, *102*, 1280.
[28] J. Zhang, Y. Liu, Y. Ke, H. Yan, *Nano Lett.* **2006**, *6*, 248.
[29] D. Nykypanchuk, M. M. Maye, D. van der Lelie, O. Gang, *Langmuir* **2007**, *23*, 6305.
[30] B. r. M. Reinhard S. Sheikholeslami, A. Mastroianni, A. P. Alivisatos, J. Liphardt, *Proc. Natl. Acad. Sci. USA* **2007**, *104*, 2667.
[31] http://www.nist.gov/mml/biochemical/bioassay/fluorescence_raman_intensity_standards.cfm.
[32] K. Lee, J. Irudayaraj, *J. Phys. Chem. C* **2009**, *113*, 5980.
[33] K. L. Wustholz, A.-I. Henry, J. M. McMahon, R. G. Freeman, N. Valley, M. E. Piotti, M. J. Natan, G. C. Schatz, R. P. V. Duyne, *J. Am. Chem. Soc.* **2010**, *132*, 10903.
[34] E. C. Le Ru, J. Grand, N. Félidj, J. Aubard, G. Lévi, A. Hohenau, J. R. Krenn, E. Blackie, P. G. Etchegoin, *J. Phys. Chem. C* **2008**, *112*, 8117.
[35] J. McMahon, A.-I. Henry, K. Wustholz, M. Natan, R. Freeman, R. Van Duyne, G. Schatz, *Anal. Bioanal. Chem.* **2009**, *394*, 1819.
[36] T. Itoh, K. Hashimoto, Y. Ozaki, *Appl. Phys. Lett.* **2003**, *83*, 2274.
[37] A. Barhoumi, D. Zhang, N. J. Halas, *J. Am. Chem. Soc.* **2008**, *130*, 14040.
[38] K. Kneipp, Y. Wang, H. Kneipp, L. T. Perelman, I. Itzkan, R. R. Dasari, M. S. Feld, *Phys. Rev. Lett.* **1997**, *78*, 1667.
[39] L. J. Harris, E. Skaletsky, A. McPherson, *J. Mol. Biol.* **1998**, *275*, 861.
[40] C. A. Mirkin, R. L. Letsinger, R. C. Mucic, J. J. Storhoff, *Nature* **1996**, *382*, 607.
[41] A. P. Alivisatos, K. P. Johnsson, X. Peng, T. E. Wilson, C. J. Loweth, M. P. Bruchez, P. G. Schultz, *Nature* **1996**, *382*, 609.
[42] R. Elghanian, J. J. Storhoff, R. C. Mucic, R. L. Letsinger, C. A. Mirkin, *Science* **1997**, *277*, 1078.
[43] L. Sun, C. Yu, J. Irudayaraj, *Anal. Chem.* **2007**, *79*, 3981.
[44] D.-K. Lim, K.-S. Jeon, H. M. Kim, J.-M. Nam, Y. D. Suh, *Nat. Mater.* **2010**, *9*, 60.
[45] M. M. Maye, D. Nykypanchuk, M. Cuisinier, D. van der Lelie, O. Gang, *Nat. Mater.* **2009**, *8*, 388.
[46] X. Qian, X.-H. Peng, D. O. Ansari, Q. Yin-Goen, G. Z. Chen, D. M. Shin, L. Yang, A. N. Young, M. D. Wang, S. Nie, *Nat. Biotechnol.* **2008**, *26*, 83.
[47] K. G. Ray, R. L. McCreery, *Appl. Spectrosc.* **1997**, *51*, 108.

Received: August 13, 2012
Published online: December 27, 2012

